suppressive products by both monocytes and mycobacteria (*16*), and the generation of suppressor T cells (*17*). In the system we describe, the chronically infected macrophages are not suppressive and express normal amounts of class II HLA-DR,DP,DQ (*10*) but do not present viable growing organisms. One mechanism could be that mycobacteria in the cell stop secreting proteins that act as strong antigens for T cells. This seems unlikely because our T cell clones respond to antigens in both the cell wall and culture filtrate (legend to Fig. 3). Alternatively, the presentation of antigens from the vacuoles containing growing mycobacteria could selectively be blocked. Acidification of vacuoles containing living virulent mycobacteria can be impaired (*18*), and this could block presentation on MHC class II products (*19*). Presentation defects could apply to other organisms that grow intracellularly and that alter phagosome-lysosome fusion and acidification (*20, 21*). The persistence of mycobacteria in macrophages has often been correlated with pathogenesis (*22*). Our findings point to another mechanism of persistence, the capacity of a growing organism to block the presentation of its own antigens.

REFERENCES AND NOTES

1. P. F. Barnes, A. B. Bloch, P. T. Davidson, D. E. Snider, Jr., *N. Engl. J. Med.* **324**, 1644 (1991).
2. C. L. Daley *et al.*, *ibid.* **326**, 231 (1992).
3. T. Pedrazzini, K. Hug, J. A. Louis, *J. Immunol.* **139**, 2032 (1987).
4. C. Leveton *et al.*, *Infect. Immun.* **57**, 390 (1989).
5. A. A. Izzo and R. J. North, *J. Exp. Med.* **176**, 581 (1992).
6. J. R. Lamb *et al.*, *Rev. Infect. Dis.* **11**, S443 (1989).
7. G. A. W. Rook, J. Steele, S. Barnass, J. Mace, J. L. Stanford, *Clin. Exp. Immunol.* **63**, 105 (1986).
8. Monocytes were isolated from Ficoll-Hypaque–selected blood mononuclear cells by adherence to plastic. The culture medium in all experiments was RPMI 1640 plus 5% heat-inactivated human serum and gentamicin (20 μg/ml). The adherent monolayer was incubated with live *M. bovis* BCG (five bacteria per cell; Trudeau Institute, Saranac Lake, NY) for 16 to 18 hours. Then we dislodged the monocytes by pipetting them, washed them free of nonbound organisms by centrifugation at 150*g* at 4°C, and cultured them an additional day (day 2, acutely infected) or 6 days (day 7, chronically infected). To stimulate DNA synthesis in T cells, we added infected macrophages (2.5×10^4) to 96-well, flat-bottomed microtest trays (Costar, Cambridge, MA) and washed the cells three times with RPMI 1640. For cytologic studies, we plated the macrophages (2×10^4 to 5×10^4) in eight-well chamber slides (Permanox Lab Tek; Nunc, Naperville, IL). Slides were air-dried before fixation in 10% formalin–phosphate-buffered saline. Mycobacteria were visualized with the fluorescent auramine-rhodamine stain (*11*).
9. We enriched T cells from individuals infected with tuberculosis or vaccinated with BCG from mononuclear cells by the formation of rosettes with neuraminidase-treated sheep erythrocytes (E rosette positive; Er^+), followed by reaction with immunoglobulin-coated dishes to deplete residual monocytes (*23*). In some cases, we enriched the $CD4^+$ subset by removing cells expressing CD8 and MHC class II molecules [B cells, monocytes, and dendritic cells (*23*)]. T cells from both individuals with tuberculosis and those vaccinated with BCG behaved similarly in our tests.
10. P. Pancholi, A. Mirza, N. Bhardwaj, R. M. Steinman, unpublished data.
11. P. Pancholi, R. M. Steinman, N. Bhardwaj, *Immunology* **76**, 217 (1992).
12. V. Kindler, A.-P. Sappino, G. E. Grau, P.-F. Piguet, P. Vassalli, *Cell* **56**, 731 (1989).
13. V. Bhardwaj and M. J. Colston, *Eur. J. Immunol.* **18**, 691 (1988).
14. P. H. Lagrange and B. Hurtrel, in Mycobacterium tuberculosis*: Interactions with the Immune System*, M. Bendinelli and H. Friedman, Eds. (Plenum, New York, 1988), pp. 171–205.
15. G. M. Bahr, G. A. W. Rook, J. L. Stanford, *Immunology* **44**, 593 (1981).
16. H. Fujiwara, K. Ohnishi, S. Kishimoto, J. J. Ellner, I. Tsuyuguchi, *ibid.* **72**, 194 (1991); J. J. Ellner and R. S. Wallis, *Rev. Infect. Dis.* **11**, S455 (1989); J. J. Ellner, *J. Immunol.* **121**, 2573 (1978).
17. R. Turcotte, *Infect. Immun.* **34**, 315 (1981); R. M. Nakamura and T. Tokunaga, in Mycobacterium tuberculosis*: Interactions with the Immune System*, M. Bendinelli and H. Friedman, Eds. (Plenum, New York, 1988), pp. 227–241.
18. A. J. Crowle, R. Dahl, E. Ross, M. H. May, *Infect. Immun.* **59**, 1823 (1991).
19. F. M. Brodsky and L. E. Guagliardi, *Annu. Rev. Immunol.* **9**, 707 (1991).
20. M. A. Horwitz and F. R. Maxfield, *J. Cell Biol.* **99**, 1936 (1984).
21. L. D. Sibley, E. Weidner, J. L. Krabenbuhl, *Nature* **315**, 416 (1985).
22. A. M. Dannenberg, Jr., in *The Mycobacteria: A Sourcebook*, G. P. Kubica and L. G. Wayne, Eds. (Dekker, New York, 1984), pp. 721–760.
23. P. Pancholi, R. M. Steinman, N. Bhardwaj, *Clin. Exp. Immunol.* **85**, 349 (1991).

24. We thank P. Brennan for *M. tuberculosis* Erdman fractions and V. Schauf, W. Rom, the staff of the Rockefeller University Hospital, and J. Adams. Supported by grants AI24775 (to R.M.S.) and AR39552 (to N.B.) from the NIH, the New York Arthritis Chapter, a Heiser Fellowship (to P.P.), the Kaskel Fund, the Llewellyn Burchell Charitable Trust, and Clinical Research Center grant MOI-RR00102.

23 December 1992; accepted 26 February 1993

CD19 of B Cells as a Surrogate Kinase Insert Region to Bind Phosphatidylinositol 3-Kinase

David A. Tuveson, Robert H. Carter, Stephen P. Soltoff, Douglas T. Fearon

Antigen receptors on B and T lymphocytes transduce signals by activating nonreceptor protein tyrosine kinases (PTKs). A family of receptor PTKs contains kinase insert regions with the sequence tyrosine-X-X-methionine (where X is any amino acid) that when phosphorylated mediate the binding and activation of phosphatidylinositol 3-kinase (PI 3-kinase). The CD19 membrane protein of B cells enhances activation through membrane immunoglobulin M (mIgM) and was found to contain a functional analog of the kinase insert region. Ligation of mIgM induced phosphorylation of CD19 and association with PI 3-kinase. Thus, CD19 serves as a surrogate kinase insert region for mIgM by providing the means for PI 3-kinase activation by nonreceptor PTKs.

The response of B lymphocytes to antigens is mediated by receptors that induce the proliferation and differentiation of these cells. The paradigm of signal transduction through antigen receptors is that of certain receptor PTKs (*1*), such as the platelet-derived growth factor (PDGF) receptor, that have two regions essential for inducing cell growth: the PTK domains that mediate intra- and intermolecular phosphorylation of tyrosines and the kinase insert regions in which autophosphorylated tyrosines that have the motif Tyr-X-X-Met (where X is any amino acid) mediate the binding and activation of PI 3-kinase (*2, 3*), an enzyme that phosphorylates phosphatidylinositol (PI) in the position of the inositol ring. One of the subunits of PI 3-kinase, p85, contains two Src homology-2 domains specific for phosphotyrosines in the Tyr-X-X-Met motif (*3, 4*). Mutation of the tyrosines in the two Tyr-X-X-Met motifs in the kinase insert region of the PDGF receptor eliminates the binding and activation of PI 3-kinase and the growth-inducing activity of the receptor (*3*).

Antigen receptors lack these functional cytoplasmic domains of the receptor PTKs but are coupled indirectly to nonreceptor PTKs (*5*) through association with other membrane proteins that share conserved cytoplasmic motifs (*6*). Nonreceptor PTKs have been suggested to interact with PI 3-kinase (*7, 8*), but members of the Src family lack phosphotyrosines with a Tyr-X-X-Met motif, and the interaction may involve other proteins (*9*).

CD19 is a B cell–specific membrane protein that is 95 kD (*10*) and that when coligated with mIgM reduces the number of antigen receptors that must be ligated to activate B cells by two orders of magnitude (*11*) and that also associates with comple-

D. A. Tuveson, Department of Molecular Biology and Genetics, Johns Hopkins University School of Medicine, Baltimore, MD 21205.
R. H. Carter, Department of Medicine, Johns Hopkins University School of Medicine, Baltimore, MD 21205.
S. P. Soltoff, Division of Signal Transduction, Department of Medicine, Beth Israel Hospital, Harvard Medical School, Boston, MA 02115.
D. T. Fearon, Department of Medicine and Department of Molecular Biology and Genetics, Johns Hopkins University School of Medicine, Baltimore, MD 21205.

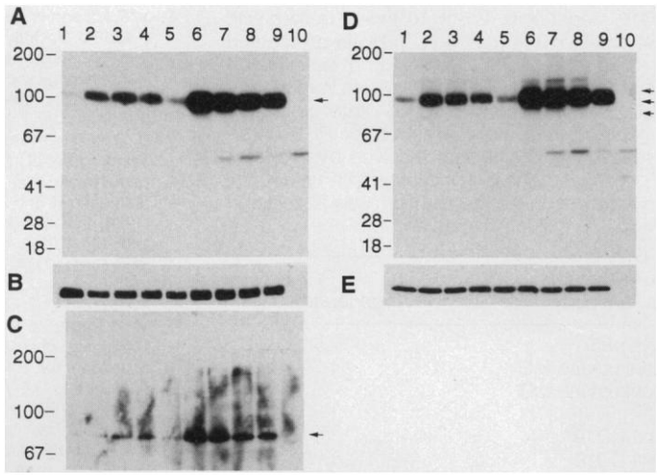

Fig. 1. Association of PI 3-kinase and tyrosine-phosphorylated CD19. (**A**) Tyrosine phosphorylation of CD19. Daudi cells (2×10^7) were treated with buffer (lane 1), biotin-conjugated monoclonal antibody (mAb) B4 to CD19 (biotin-B4; 4 μg/ml) (*11*) (lanes 2 to 5), biotin-conjugated Fab′ of mAb DA4.4 anti-IgM (biotin-DA4.4; 1 μg/ml) (*11*) (lanes 6 to 9), and biotin-B4 and biotin-DA4.4 Fab′ together (lane 10). Cells were incubated at 20°C with avidin for 1 min (lanes 2 and 6), 5 min (lanes 3 and 7), 15 min (lanes 4, 8, and 10), and 45 min (lanes 5 and 9). NP-40 lysates were immunoprecipitated with rabbit anti-CD19 (arrowhead) (lanes 1 to 9) or nonimmune IgG (lane 10); the precipitated proteins were probed on protein immunoblots (*25*) with ^{125}I-labeled 4G10 mAb to phosphotyrosine. (**B**) Recovery of CD19. The blot in (A) was reprobed with rabbit anti-CD19 and peroxidase-conjugated mouse antibodies to rabbit IgG, which were detected by ECL. (**C**) Coprecipitation of p85 with anti-CD19. A replicate of the blot in (A) was probed with anti-p85 (arrowhead), which was detected by ECL. (**D**) Coprecipitation of tyrosine-phosphorylated CD19 with anti-p85. Replicate samples of the lysates from Daudi cells prepared as described in (A) were immunoprecipitated with anti-p85 (lanes 1 to 9) or nonimmune antibody (lane 10), and the precipitated proteins were analyzed by protein immunoblotting with ^{125}I-labeled 4G10. The arrows indicate specifically coprecipitating proteins. (**E**) Recovery of p85. The blot in (D) was reprobed with anti-p85, which was detected by ECL. Molecular size standards are indicated at left in kilodaltons.

ment receptor type 2 (CR2; CD21) to augment the immune response (*12*). Two sites in the cytoplasmic domain of CD19, Tyr^{484}-Glu-Asp-Met and Tyr^{515}-Glu-Asn-Met, exhibit the Tyr-X-X-Met motif. We therefore determined whether CD19 serves as a surrogate kinase insert region by recruiting PI 3-kinase for the nonreceptor PTKs that are activated by mIgM.

We investigated the ability of CD19 to be phosphorylated on tyrosine (tyrosine-phosphorylated) and to bind PI 3-kinase. Lysates were made of Daudi B cells on which CD19 and mIgM had been cross-linked, and immunoprecipitates were formed with antibodies specific to CD19 (anti-CD19). Immunoblots were probed with antibodies specific to phosphotyrosine (anti-phosphotyrosine), CD19, and p85 (anti-p85). Cross-linking CD19 or mIgM increased tyrosine phosphorylation of CD19 within 1 min; this increase persisted for 45 min and was greater in cells on which mIgM had been ligated (Fig. 1, A and B). The presence of phosphotyrosine in CD19 was verified by phosphoamino acid analysis. The p85 subunit of PI 3-kinase coprecipitated with anti-CD19 in parallel with the intensity of tyrosine phosphorylation of CD19 (Fig. 1C).

The major tyrosine-phosphorylated protein coprecipitating with p85 in B cells activated through the antigen receptor was CD19 (Fig. 1, D and E). The identity of the coprecipitating 95-kD protein as CD19 was confirmed by its depletion when lysates were first cleared with anti-CD19. Half of the tyrosine-phosphorylated CD19 was associated with p85 when lysates of Daudi cells on which mIgM had been ligated were first cleared with anti-p85, and residual tyrosine-phosphorylated CD19 was assayed by immunoprecipitation with anti-CD19 and protein immunoblotting with antibodies to phosphotyrosine (anti-phosphotyrosine).

Recombinant p85, when used as a probe for immunoblots, bound directly to CD19 that had been immunoprecipitated from B cells activated through mIgM. The interaction was abolished by tyrosine dephosphorylation of CD19 by phosphotyrosine phosphatase–1B (PTP-1B) (*13*) (Fig. 2).

The tyrosine-phosphorylated Ig-α/Ig-β heterodimer of the mIg complex (*6*), the subunits of which are 47 and 37 kD, was not present in anti-p85 immunoprecipitates of activated B cells (Fig. 1D). We extended this finding by demonstrating that p85 did not co-immunoprecipitate with Ig-α from lysates of B cells that were resting or were activated through their antigen receptor (*14*).

Jurkat T cells were stably transfected (*15*) with wild-type CD19 and CD19-(Y484F, Y515F), a mutant form in which the tyrosines (Y) in the two Tyr-X-X-Met motifs were substituted with phenylalanine (F) (*16*). Wild-type CD19 expressed by a Jurkat T cell clone was constitutively tyrosine-phosphorylated, and the phosphorylation was slightly enhanced when these cells were optimally treated with antibody to CD3; the CD19 from these cells was associated with p85 (Fig. 3). Jurkat T cells expressing CD19(Y484F, Y515F) lacked

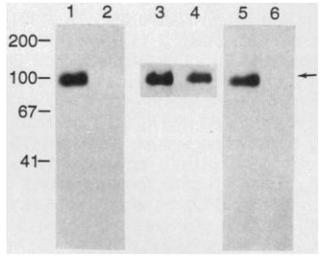

Fig. 2. Binding of recombinant p85 (*26*) to tyrosine-phosphorylated CD19. Replicate samples of anti-CD19 immunoprecipitates from Daudi cells that had been activated with biotin-DA4.4 Fab′ and avidin as described in Fig. 1 were treated with buffer (lanes 1, 3, and 5) or PTP-1B (*13*) (lanes 2, 4, and 6). Immunoblots were probed with ^{125}I-labeled 4G10 (lanes 1 and 2), anti-CD19 followed by ECL (lanes 3 and 4), or recombinant p85 followed by ECL (lanes 5 and 6). Arrowhead indicates CD19; molecular size standards are shown at left in kilodaltons.

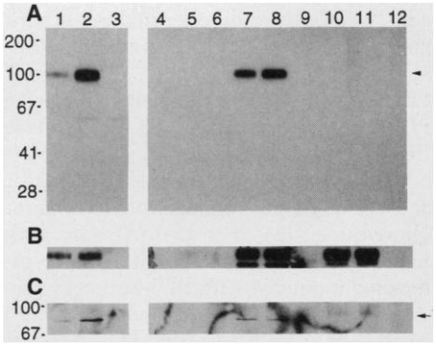

Fig. 3. Wild-type CD19 and CD19(Y484F, Y515F): tyrosine phosphorylation and association with p85. (**A**) Tyrosine phosphorylation of wild-type CD19 and CD19(Y484F, Y515F) in 1×10^7 cells. Daudi B cells (lanes 1 to 3), untransfected Jurkat T cells (lanes 4 to 6), or Jurkat T cells transfected with wild-type CD19 (lanes 7 to 9) or CD19(Y484F, Y515F) (lanes 10 to 12) were treated at 20°C for 10 min with buffer (lanes 1, 4, 7, and 10), goat F(ab′)$_2$ antibodies to human IgM (10 μg/ml) (lanes 2 and 3), or a 1:500 dilution of antibody to CD3 (OKT3 ascites) (Ortho Diagnostics, Raritan, New Jersey) (lanes 5, 6, 8, 9, 11, and 12). NP-40 lysates were immunoprecipitated with nonimmune rabbit IgG (lanes 3, 6, 9, and 12) or rabbit anti-CD19 (lanes 1, 2, 4, 5, 7, 8, 10, and 11), and immunoblots were probed with ^{125}I-labeled 4G10 anti-phosphotyrosine to reveal tyrosine-phosphorylated CD19 (arrowhead). (**B**) Recovery of CD19. The blot in (A) was reprobed with anti-CD19, which was detected by ECL. (**C**) Coprecipitation of p85. A replicate blot was probed with anti-p85 (indicated by the arrowhead), which was detected by ECL. Molecular size standards are shown at left in kilodaltons.

Table 1. PI 3-kinase activity associated with anti-CD19. Daudi cells (2.5×10^7) were treated with buffer, biotin-conjugated mAb B4 to CD19 (biotin-B4 anti-CD19; 4 μg/ml) (*12*), biotin-conjugated Fab′ of mAb DA4.4 to IgM (biotin-DA4.4 anti-IgM; 1 μg/ml) (*11*), or biotin-B4 and biotin-DA4.4 together. Cells were incubated with avidin for 10 min at 20°C, and NP-40 lysates were immunoprecipitated with nonimmune rabbit IgG or rabbit anti-CD19; lysates from 0.5×10^7 Daudi cells were also immunoprecipitated with anti-p85. The immunoprecipitates were assayed for PI 3-kinase activity with PI as the substrate (*17, 18*), and the reaction products were resolved by thin-layer chromatography. The incorporation of $^{32}PO_4$ into the phosphatidylinositol phosphate (PIP) products, which were shown by HPLC analysis to be phosphorylated only in the D-3 position, was quantitated with a Betascope (Betagen, Waltham, Massachusetts).

Treatment of B cells	Precipitating antibody	PI-3-P generated (cpm)
Buffer	Anti-p85	519
Buffer + avidin	Nonimmune IgG	3
Biotin-B4 anti-CD19 + biotin-DA4.4 anti-IgM + avidin	Nonimmune IgG	2
Buffer + avidin	Anti-CD19	4
Biotin-B4 anti-CD19 + avidin	Anti-CD19	30
Biotin-DA4.4 anti-IgM + avidin	Anti-CD19	134

both characteristics (Fig. 3). Therefore, Tyr^{484}, Tyr^{515}, or both are substrates for PTKs in Jurkat T cells and mediate the binding by CD19 of PI 3-kinase. Similar results were observed in two other Jurkat clones expressing CD19(Y484F, Y515F).

PI 3-kinase activity, as assessed by the conversion of PI to phosphatidylinositol 3-phosphate (PI-3-P) (*17, 18*), coprecipitated with CD19 from lysates of Daudi cells that had been treated with anti-CD19 or antibody to IgM (anti-IgM), with four times more activity being recovered from the latter (Table 1). Therefore, the catalytic p110 subunit of the PI 3-kinase also was associated with tyrosine-phosphorylated CD19.

This function of CD19 may account for the activation of PI 3-kinase by the ligation of mIgM, and possibly of CD19, on the intact B cell. In three of three experiments, ligating mIgM on Daudi cells labeled with inorganic ^{32}P generated amounts of phosphatidylinositol 3,4-bisphosphate (PI-3,4-P_2) that were 4.9%, 7.8%, and 6.9% of the total cellular phosphatidylinositol bisphosphate (PIP_2); phosphatidylinositol 3,4,5-trisphosphate (PI-3,4,5-P_3) was not detected (*19, 20*). In only one of these experiments did ligation of CD19 generate detectable PI-3,4-P_2, which was 2.0% of total PIP_2, consistent with the smaller amount of PI 3-kinase associated with CD19 in cells so treated (Fig. 1 and Table 1).

Cross-linking mIg enables PI 3-kinase activity to be precipitated with anti-phosphotyrosine (*18*) or to Lyn (*8*). Our findings suggest that anti-phosphotyrosine interacted indirectly with PI 3-kinase by precipitating tyrosine-phosphorylated CD19; we did not observe a tyrosine-phosphorylated protein of 55 KD, the molecular size of Lyn, coprecipitating with anti-p85 (Fig. 1D). Although the cytoplasmic domains of Ig-α and Ig-β may interact with PI 3-kinase (*21*), these proteins did not co-immunoprecipitate with PI 3-kinase (Fig. 1D) (*14*), which suggests that p85 interacts more stably with tyrosine-phosphorylated CD19.

The interaction of CD19 with PI 3-kinase is distinct from that of polyoma middle T antigen (*9, 22*) and IRS-1 (*23*), two other proteins that lack PTK activity and bind PI 3-kinase, in that CD19 is capable of directly localizing PI 3-kinase to the membrane, a step that may be necessary for the function of the enzyme (*24*). This capability of CD19, which is analogous to that of the kinase insert region of receptor PTKs, is likely to be relevant to the recognition of antigen by B cells because it is elicited by mIgM.

REFERENCES AND NOTES

1. M. R. Gold, D. A. Law, A. L. DeFranco, *Nature* **345**, 810 (1990); M. Campbell and B. Sefton, *EMBO J.* **9**, 2125 (1990).
2. J. A. Escobedo and L. T. Williams, *Nature* **335**, 85 (1988); S. R. Coughlin, J. A. Escobedo, L. T. Williams, *Science* **243**, 1191 (1989); A. Kazlauskas and J. A. Cooper, *Cell* **58**, 1121 (1989); L. Varticovski, B. Drucker, D. Morrison, L. Cantley, T. Roberts, *Nature* **342**, 699 (1989); M. Reedijk, X. Liu, T. Pawson, *Mol. Cell. Biol.* **10**, 5601 (1990); S. A. Shurtleff *et al.*, *EMBO J.* **9**, 2415 (1990); L. C. Cantley *et al.*, *Cell* **64**, 281 (1991); A. Kazlauskas, A. Kashishian, J. Cooper, M. Valius, *Mol. Cell. Biol.* **12**, 2534 (1992); S. Lev, D. Givol, Y. Yarden, *Proc. Natl. Acad. Sci. U.S.A.* **89**, 678 (1992).
3. W. J. Fantl *et al.*, *Cell* **69**, 413 (1992).
4. J. A. Escobedo *et al.*, *ibid.* **65**, 75 (1991); M. Otsu *et al.*, *ibid.*, p. 91; E. Y. Skolnik *et al.*, *ibid.*, p. 83.
5. A. L. Burkhardt, M. Brunswick, J. B. Bolen, J. J. Mond, *Proc. Natl. Acad. Sci. U.S.A.* **88**, 7410 (1991); Y. Yamanishi, T. Kakiuchi, J. Mizuguchi, T. Yamamoto, K. Toyoshima, *Science* **251**, 192 (1991); M. Campbell and B. M. Sefton, *Mol. Cell. Biol.* **12**, 2315 (1992); T. Taniguchi *et al.*, *J. Biol. Chem.* **266**, 15790 (1991); J. E. Hutchcroft, M. L. Harrison, R. L. Geahlen, *ibid.* **267**, 8613 (1992).
6. M. Reth, *Nature* **338**, 383 (1989); K. S. Campbell and J. C. Cambier, *EMBO J.* **9**, 441 (1990); J. Hombach, T. Tsubata, L. Leclercq, H. Stappert, M. Reth, *Nature* **343**, 760 (1990); M. R. Gold, L. Matsuuchi, R. B. Kelly, A. L. DeFranco, *Proc. Natl. Acad. Sci. U.S.A.* **88**, 3436 (1991); C. J. M. van Noesel *et al.*, *J. Immunol.* **146**, 3881 (1991); A. R. Venkitaraman, G. T. Williams, P. Dariavach, M. S. Neuberger, *Nature* **352**, 777 (1991).
7. Y. Fukui and H. Hanafusa, *Mol. Cell. Biol.* **9**, 1651 (1989); J. S. Gutkind, P. M. Lacal, K. C. Robbins, *ibid.* **10**, 3806 (1990); M. C. O'Brien, Y. Fukui, H. Hanafusa, *ibid.*, p. 2855.
8. Y. Yamanishi *et al.*, *Proc. Natl. Acad. Sci. U.S.A.* **89**, 1118 (1992).
9. D. R. Kaplan *et al.*, *ibid.* **83**, 3624 (1986); D. A. Talmadge *et al.*, *Cell* **59**, 55 (1989).
10. L. M. Nadler *et al.*, *J. Immunol.* **131**, 244 (1983); I. Stamenkovic and B. Seed, *J. Exp. Med.* **168**, 1205 (1988); T. F. Tedder and C. M. Isaacs, *J. Immunol.* **143**, 712 (1989).
11. R. H. Carter, D. A. Tuveson, D. J. Park, S. G. Rhee, D. T. Fearon, *J. Immunol.* **147**, 3663 (1991); R. H. Carter and D. T. Fearon, *Science* **256**, 105 (1992).
12. M. B. Pepys, *J. Exp. Med.* **140**, 126 (1974); A. K. Matsumoto *et al.*, *ibid.* **173**, 55 (1991); B. Heyman, E. J. Wiersma, T. Kinoshita, *ibid.* **172**, 665 (1990); T. Hebell, J. M. Ahearn, D. T. Fearon, *Science* **254**, 102 (1991).
13. CD19 that had been released from immobilized anti-CD19 by heating at 100°C for 10 min in 20 mM Hepes, pH 7.3, was incubated for 2 hours at 37°C with 12.5 μg of the glutathione-S-transferase–PTP-1B fusion protein coupled to Sepharose (UBI, Lake Placid, NY) [J. V. Frangioni, P. H. Beahm, V. Shifrin, C. A. Jost, B. G. Neel, *Cell* **68**, 545 (1992)].
14. D. A. Tuveson and D. T. Fearon, unpublished data.
15. The Jurkat human T cell leukemia line was electroporated [B. A. Irving and A. Weiss, *Cell* **64**, 891 (1991)] with plasmids encoding either wild-type CD19 or CD19(Y484F, Y515F), and clones were screened for CD19 expression by flow cytometry (FACScan; Becton-Dickinson).
16. The Bam HI–Bam HI fragment of pZipneo.SV(CD19) (*12*) containing CD19 cDNA was cloned into the pALTER-1 vector (Promega, Madison, WI). The TAT codons for Tyr^{484} and Tyr^{515} were converted by site-directed mutagenesis to TTT (Phe) by use of the synthetic oligonucleotides GTCCCAGTCCTTTGAGGATATGAGA and AGATGCAGACTCTTTTGAGAACATGGA, which contain 10 to 12 bases of appropriate sequence flanking the central mismatch. The fragment encoding the Y484F and Y515F substitutions, as determined by DNA sequencing, was then cloned back into pZipneo.SV.
17. M. Whitman, D. R. Kaplan, B. Schaffhausen, L. Cantley, T. M. Roberts, *Nature* **315**, 239 (1985).
18. M. R. Gold, V. W. Chan, C. W. Turck, A. L. DeFranco, *J. Immunol.* **148**, 2012 (1992).
19. K. R. Auger, L. A. Serunian, S. P. Soltoff, P. Libby, L. C. Cantley, *Cell* **57**, 167 (1989).
20. L. A. Serunian, K. A. Auger, L. C. Cantley, *Methods Enzymol.* **198**, 78 (1991).
21. M. R. Clark *et al.*, *Science* **258**, 123 (1992).
22. S. A. Courtneidge and A. Heber, *Cell* **50**, 1031 (1987); D. R. Kaplan *et al.*, *ibid.*, p. 1021.
23. X. J. Sun *et al.*, *Nature* **352**, 73 (1991); J. M. Backer *et al.*, *EMBO J.* **11**, 3469 (1992).
24. L. Vartikovski, G. Q. Daley, P. Jackson, D. Baltimore, L. C. Cantley, *Mol. Cell. Biol.* **11**, 1107 (1991).
25. Cell pellets were lysed in 1% NP-40, 50 mM tris, 10 mM EDTA, 80 mM KCl, 10 mM MoO_4, 1 mM VO_4, 5 mM iodoacetamide, leupeptin (10 μg/ml), aprotinin (10 μg/ml), aminoethylbenzenesulfonylfluoride (10 μg/ml), *p*-nitrophenyl-*p*′-guanidinobenzoate (10 μg/ml), antipain (1 μg/ml), pepstatin (1 μg/ml), chymostatin (1 μg/ml), and diisopropylfluorophosphate (5 mM), pH 7.5. Anti-CD19 was produced by the injection of rabbits with a recombinant fusion protein containing amino acids 310 to 540 of the cytoplasmic portion of human CD19 joined to the COOH-terminus of maltose-binding protein (New England Biolabs, Beverly, MA). Immunoprecipitates were resolved on reducing SDS–8% polyacrylamide gels (SDS-PAGE) and transferred to nitrocellulose. The filters were processed (*11*), and monoclonal antibody (mAb) 4G10 (anti-phosphotyrosine) (UBI) was directly labeled with ^{125}I. Film (XARS; Kodak) was exposed to the dried filters at −80°C with an intensifying screen. Filters that were reprobed were incubated with a 1:5000 dilution of anti-CD19 or anti-p85 (UBI), washed, incubated with a

1:10,000 dilution of peroxidase-conjugated mouse antibody to rabbit IgG (Jackson ImmunoResearch), washed, and developed with enhanced chemiluminescence (ECL) (Amersham). The exposure times needed for ECL detection ranged from 10 s to 5 min, a period of time too brief to detect signals from bound ^{125}I.
26. CD19-containing immunoprecipitates were resolved by SDS-PAGE and transferred to nitrocellulose filters. We used lysates of *Escherichia coli* containing recombinant p85 fused to the epitope tag KT3 at a protein concentration of 1 μg/ml to probe blocked nitrocellulose filters [A. Klippel, J. Escobedo, W. Fantl, L. Williams, *Mol. Cell. Biol.* 12, 1451 (1992)]. The filters were sequentially incubated with a 1:1250 dilution of mouse antibodies to KT3 and peroxidase-conjugated rabbit antibodies to mouse IgG (Jackson ImmunoResearch) and then developed with the ECL reagent.
27. We thank B. Drucker for the 4G10 antibody, A. Klippel and L. Williams for the p85-KT3 recombinant protein and the antibody to KT3, A. Choi for assistance with the Betascope, and L. Cantley for the use of his high-performance liquid chromatography (HPLC) facility. Supported by grants AI22833 and AI28191 from the National Institute of Allergy and Infectious Diseases of NIH (to D.T.F.), by the Medical Scientist Training Program (number 5T32GM07309 to D.A.T.), and by the Arthritis Foundation (to R.H.C.).

22 December 1992; accepted 25 February 1993

Localization of a Memory Trace in the Mammalian Brain

David J. Krupa,* Judith K. Thompson, Richard F. Thompson

The localization of sites of memory formation within the brain has proven to be a formidable task even for simple forms of learning and memory. In order to localize a particular site of memory formation within the brain, the rabbit eyeblink response was classically conditioned while regions of the cerebellum or red nucleus were temporarily inactivated by microinfusions of the γ-aminobutyric acid agonist muscimol. Cerebellar inactivation completely blocked learning but had no effect on subsequent learning after inactivation, whereas red nucleus inactivation did not prevent learning but did block the expression of conditioned responses. The site of memory formation for this learned response thus appears to be localized within the cerebellum.

A primary goal of neuroscience and psychology is to acquire an understanding of the mechanisms that underlie long-term memory formation, storage, and retrieval in the mammalian, particularly the human, brain (*1*). An essential prerequisite is identification of the sites within the brain where particular memories, either distributed or localized, are created and stored (the memory trace). To date, precise identification of loci for memory storage has remained elusive (*2*, *3*). We report here evidence for localization of a long-term memory trace in the mammalian brain, specifically within the cerebellum.

We used local microinfusions of the γ-aminobutyric acid (GABA) agonist muscimol to reversibly inactivate select regions of the brain during the training of rabbits in order to localize the memory trace. Muscimol is known to temporarily inhibit activity of neurons that express $GABA_A$ receptors by hyperpolarizing somata and dendrites by increasing a Cl^- conductance (*4*). Muscimol has been used for reversible inactivation of brain regions, including the cerebellum (*5*) and the red nucleus (*6*), but generally has not been used to localize memory traces.

The logic underlying the use of reversible lesions to localize sites of memory formation is as follows. Naïve animals are trained while a region of the brain is inactivated. If this inactivated region is part of the circuitry essential for a given form of learning and memory, then expression of any learned response will be prevented during the inactivation training. If learning occurs during inactivation, as evidenced by the immediate expression of learned responses in training after inactivation, then the site or sites of memory trace formation must be afferent (upstream) to the region of inactivation in the essential circuitry. If no learning occurs during inactivation training, then the region of inactivation must be the site of memory formation or a mandatory afferent projecting ultimately to the site of memory formation.

To utilize reversible inactivation, one must first identify the brain circuitry essential (necessary and sufficient) for a given form of learning and memory. This has largely been achieved for one form of basic associative memory in animal studies, aversive classical conditioning of discrete behavioral responses—for example, eyeblink and limb flection (*2*, *7*). In brief, the results of lesion, recording, and stimulation studies indicate that the conditioned stimulus (CS) pathway includes sensory relay nuclei, the pontine nuclei, and mossy fiber projections to the cerebellum; the unconditioned stimulus (US) pathway includes somatosensory relay nuclei, the inferior olive, and its climbing fiber projections to the cerebellum; and the conditioned response (CR) pathway includes the cerebellum, its projection from the interpositus nucleus to the red nucleus, and red nucleus projections to premotor and motor nuclei (*8*, *9*). Unilateral cerebellar lesions in humans completely prevent learning of the eyeblink CR ipsilateral (but not contralateral) to the lesion (*10*).

We used microinfusions of muscimol into the ipsilateral lateral cerebellum or the contralateral red nucleus to temporarily inactivate these structures during acquisition of the classically conditioned eyeblink response of the rabbit. Behavioral training comprised 11 daily sessions in which a tone CS (350 ms, 1 KHz, 85 dB) was paired with a coterminating corneal airpuff US (100 ms, 2.1 N/cm^2) (*11*). One hour before each of the first six sessions, animals received an infusion of (i) muscimol into the ipsilateral lateral cerebellum ($n = 6$), (ii) saline (vehicle) into the ipsilateral lateral cerebellum ($n = 6$), or (iii) muscimol into the contralateral red nucleus ($n = 6$) (*12*). No infusions were administered on days 7 to 10 of training. All animals received 3 days of rest between sessions 6 and 7 to ensure no lingering effects of infusion. On day 11, all animals were infused with muscimol to test retention.

Control animals that were treated with saline had fully learned the CR by the third day of infusion training. Neither the animals infused with muscimol into the cerebellum nor those infused in the red nucleus showed any appreciable number of CRs during the 6 days of infusion training (Fig. 1A). At the beginning of training after the infusion sessions (day 7), the animals infused with muscimol in the cerebellum showed no signs of having learned and subsequently learned at exactly the same rate as the saline-treated control animals had learned on the first 4 days of training (Fig. 1B). In marked contrast, the animals that had had muscimol infused into the red nucleus showed asymptotic learning from the beginning of training after the infusion (Fig. 1B). Infusions of muscimol on day 11 into the cerebellum (including the control animals that had previously been infused with saline) or the red nucleus reversibly abolished the CRs of all animals. In all cases, infusions of muscimol into the cerebellum or the red nucleus during acquisition had no effect on UR amplitudes relative to controls (*13*) (Fig. 1C).

Locations of the cannula tips for all animals are shown in Fig. 2A. All cerebellar cannulae were aimed at the anterior interpositus nucleus (AIN). After all training, four animals (three infused in the cerebellum, one in the red nucleus) received infusions of [^{3}H]muscimol equiva-

Neurosciences Program, University of Southern California, Los Angeles, CA 90089.

*To whom correspondence should be addressed.